

OPTICAL PROPERTY INVESTIGATION IN SEQUENTIAL MULTI-COMPONENT MOLDING

Chao-Tsai Huang¹, Meng-Chih Chen¹, Yuan-Rong Chang¹, Wen-Li Yang¹, Shi-Chang Tseng², and Huang-Yi Chang²,

1. CoreTech System (Moldex3D) Co., Ltd., ChuPei City, Hsinchu, Taiwan

2. Dept. of Mechanical Engineering, National Yunlin University of Science & Technology.

Abstract

Sequential multi-component molding is one of great methods to fabricate the modern injection products. Previous literatures have shown that various parameters including the product geometries and molded materials will affect the warpage of final products significantly. However, how the polymer property and process effects on the optical characteristics are still not clear. In this study, we will demonstrate how the polymer viscoelastic property and process induced effects on the residual stresses. Those stresses will go further to influence the optical properties of multi-component molding products.

Introduction

In modern plastic molded product fabrication, sequential multi-component molding provides great methods to diversify the development. In fact, the fundamental idea of sequential multi-component was first proposed and patented in 1962 regarding the development of multiple material tailing light by G. Carozzo [1]. During the past decades, many new technologies, methods, and related material combination have been proposed [2-4]. In the recent years, people have tried to realize the physical mechanism and to handle this complicated process to be more understanding. However, some physical properties, such as residual stresses, birefringence, and so on, are still not clear yet [7-10]. Due to its complicated nature and the unclear physical mechanism for the sequential multi-component molding processes, a conventional trial-and-error method cannot catch the crucial factors effectively. Hence, in this study, we have applied CAE tool and techniques to get better understanding. Specifically, we have conducted the optical property of a U-type injection parts in multi-component molding systematically. Results show both flow-induced effect and thermal-induced effect will influence the residual stresses and the birefringence. Furthermore, when the dimensions (say the width) of parts change, the birefringence variation will occur with a turn-over point (around width of 0.75 mm). The turn-over point is matched with the warpage behavior as we have seen in the previous study [4, 8].

Theory Approach and Assumption

The major analysis procedures for injection molding processes include filling, package, cooling, and warpage. In filling/packing stages, the polymer melt is assumed to behave as Generalized Newtonian Fluid

(GNF). Hence the non-isothermal 3D flow motion can be mathematically described. The FVM (finite volume method), due to its robustness and efficiency, is employed in this study to solve the transient flow field in complex three-dimensional geometries. During the mold cooling stage, a three-dimensional, cyclic, transient heat conduction problem with convective boundary conditions on the cooling channel and mold base surfaces is involved. The basic mathematical models are described in detailed in Ref. [5-7].

To handle the viscoelastic behavior of polymeric melts, τ is obtained by the constitutive equation of White Metzner Model:

$$\tau + \lambda \left(\frac{\partial \tau}{\partial t} + V \cdot \nabla \tau - \nabla V^T \cdot \tau - \tau \cdot \nabla V \right) = \eta (\nabla V + \nabla V^T) \quad (1)$$

$$\eta(T, \dot{\gamma}) = \eta_0(T_f) \cdot a(T, \dot{\gamma}) \quad (2)$$

$$\lambda(T, \dot{\gamma}) = \lambda_0(T_f) \cdot a(T, \dot{\gamma}) \quad (3)$$

$$a(T, \dot{\gamma}) = \frac{\eta(T, \dot{\gamma})}{\eta_0} \quad (4)$$

where λ is the relaxation time, λ_0 is the relaxation time at zero shear rate, η is the shear viscosity, η_0 is the shear viscosity at zero shear rate, and a is shift factor.

In addition, to handle the sequential multi-component molding, the molded part (the previous shot) will be setup into the cavity to become the boundary for the next shot. The geometry of 1st shot is assumed as a perfect U-type shape. The overall heat transfer phenomenon is governed by a three-dimensional Poisson equation. We assume there is a cycle-averaged mold temperature that is invariant with time. The warpage analysis assumes the mechanical properties are linear elasticity. The stress-strain equilibrium equations enable us to solve the problems. Also, the interfacial adhesion between sequential shots is assumed perfect.

Furthermore, to predict the optical property in plastics, the mathematical models and equations, including Stress-Optics (or Brewster's Law) for birefringence, retardation definition, and fringe order prediction, are described in detailed in our previous paper (please see Ref. [7]).

Investigation Procedures

To get better understanding of residual stresses and optical property of parts in sequential multi-component molding processes, firstly, we have conducted using Moldex3D[®] software numerically.

The geometrical model which includes runner system and dimensions is as shown in Fig. 1 and 2. The dimension of 1st shot, or insert, is 19mm X 9.5mm X 2mm. The dimension of 2nd shot is (19+2x)mm X (9.5+2x)mm X 2mm, where x is from 0.25 to 2 mm. The materials of 1st shot or 2nd shot in this study are ABS, PC, or PMMA. Here, ABS is Chi-Mei Polylac PA-777D, PC is GE Lexan 141, and PMMA is Chi-Mei CM-211. In this asymmetrical (U-type) structure, the solid constraints on the models with inserts are displayed. Fig. 2 shows the runner structure and the moldbase, including cooling channel layout. To perform optical property prediction, the stress-optical coefficients are around $1.0e^{-10}$ to $5.0e^{-9}$ (1/Pa) [10].

Results and Discussions

Fig. 3 shows the filling behaviors of 2nd shot in the sequential multi-component molding. Since the filling time is short, the filling behavior looks not very different from that in a single shot system. However, in the presence of 1st shot, the temperature distribution is significant different from that in a single shot system during cooling phase [8]. Fig. 4 displays the shear stress at the end of filling. It is clear that the high shear areas appear near the solid boundaries. It is mainly due to shearing of melt. After being cooled down, the principal stresses at main flow directions are evaluated suitably in Fig. 5. Basically, birefringence is proportional to principal stress difference. The flow-induced birefringence can be computed and is obtained in Fig. 6 (a). Additionally, Fig 6 (b) and (c) show the thermal-induced and total birefringence, respectively. In this case, the thermal-induced effect dominates the optical properties. Furthermore, to predict the optical property of parts, the fringed pattern can help people quickly evaluate qualitatively. Fig. 7 (a) and (b) show the flow-induced and thermal-induced effects respectively. Total effect is displayed in Fig. 7 (c).

To realize the relationship between polymeric behavior and optical property along the geometrical structure, we have systematically conducted various dimensions. Firstly, when melt flows from upstream (line A) to downstream (line D) as shown in Fig. 8, we would like to observe residual stresses and optical properties. In each line (except of A), the stresses or birefringence are obtained from 0 mm (the surface next to the mold) to 2.0 mm (the interface between melt and insert). In Fig. 9 (a), line B, C, and D, show the similar trends. The high flow-induced birefringence is developed on both sides next to solid boundaries. However, line A shows the birefringence increases from the entrance to the insert surface. Meanwhile, Fig. 9 (b) and (c) shows the

thermal-induced and total birefringence. To figure out each effect contribution, Fig. 10 shows the birefringence distribution from upstream location (line A) to downstream location (line B). Clearly, in this case, both locations show the thermal-induced effect dominates the birefringence phenomena.

Furthermore, we focus on the optical property variation with increasing width (W is defined in Fig. 1). In our previous study, when the width increases from W=0.25 mm to W=2.0 mm, the warpage tendency will change from inward to outward. The turn-over point of width is around 0.75 mm. Here, for each width, we picked up the physical property at the center point of each line. Detail is described in Fig. 8. The birefringence variation is shown in Fig. 11. The interesting phenomenon is that the flow-induced birefringence increases gradually at the beginning until it reaches the maximum value and then decreases as the width increases. At the same time, the thermal-induced birefringence decreases gradually at the beginning until it reaches the minimum value and then increases as the width increases. The turn-over point is around width of 0.75 mm. This critical point of warpage tendency is similar to what we have found in our previous study [4,8].

Conclusion

In this study, we have conducted the optical property of injection parts in sequential multi-component molding systematically. Both of flow-induced and thermal-induced contributions can be predicted and distinguished separately. Moreover, birefringence variation along the flow direction is also investigated. This birefringence will dramatically change from gate to end-of-filling. Furthermore, optical property varies as the width of the U-type model increases. The turn-over point matches the warpage behavior, as we saw before. Finally, the verification using the experimental investigation is still working on.

References

1. US patent #3,051,994.
2. Multi-material Technology, Battenfeld.
3. Web source <http://www.engelmachinery.com>
4. Chao-Tsai Huang et al, *SPE ANTEC*, 1888-1892 (2006).
5. R. Y. Chang and W. H. Yang, *International Journal for Numerical Methods in Fluids*, 37: 125-48 (2001).
6. Rong-Yeu Chang et al, *SPE ANTEC*, 496-500 (2004).
7. Yuan-Rong Chang, et al, *SPE ANTEC*, 2490-2493 (2007).
8. Chao-Tsai Huang et al, *SPE ANTEC*, 761-765 (2007).
9. A. I. Isayev and T.H. Lin, *SPE ANTEC*, 2485-2489 (2007).
10. G. D. Shyu, A. I. Isayev and T.H. Lin, *J Polym Sci, Polym Phy*, Vol. 39, 2252-2262 (2001).

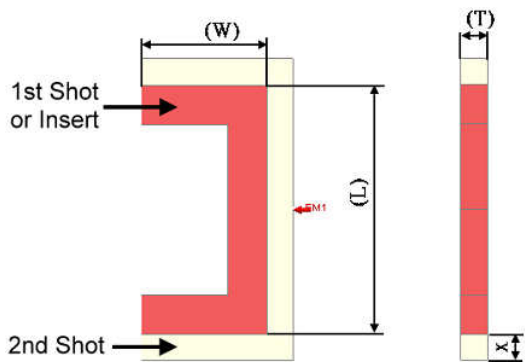


Fig. 1. The model structure and dimension: it includes the dimension and geometrical structures for 1st shot and 2nd shot.

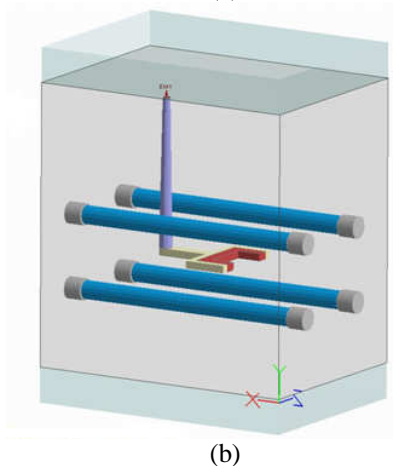
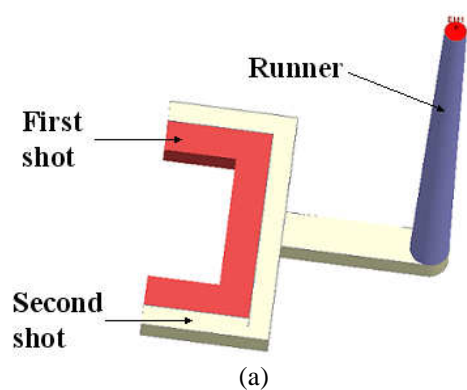


Fig. 2. System construction in this study: (a) the runner structure, (b) the cooling channel and moldbase construction.

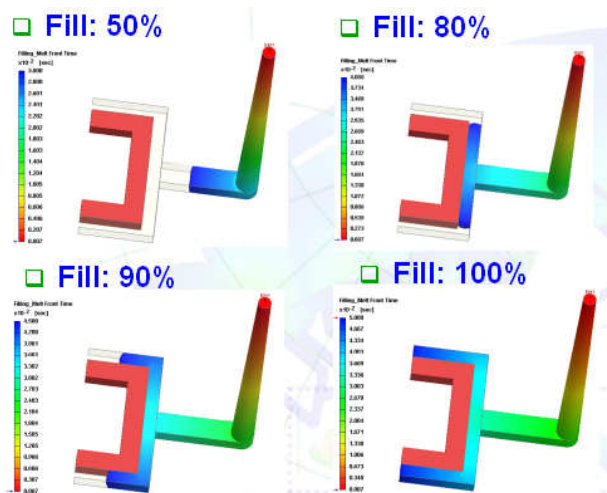


Fig. 3. The filling behaviors of the 2nd shot in sequential multi-component molding. (width of 2nd shot $x=2$ mm).

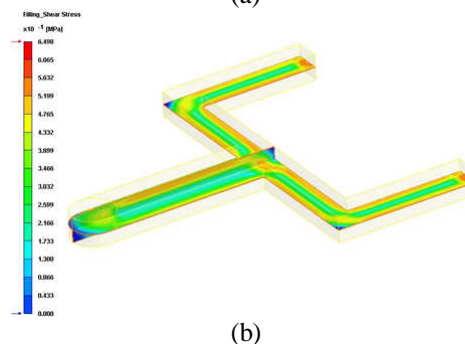
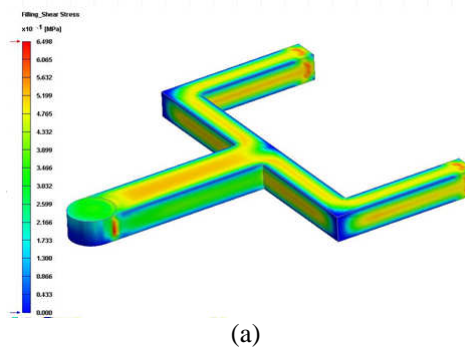
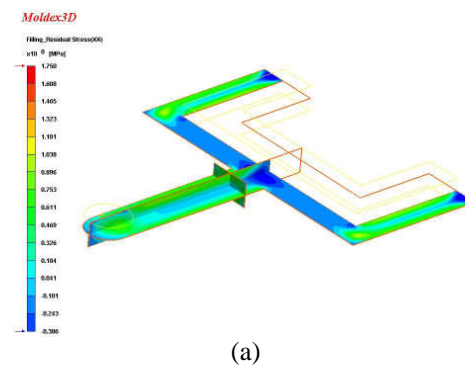


Fig. 4. The shear stresses at the end of filling: (a) view from part surface, (b) view from inner sliced planes.



(a)

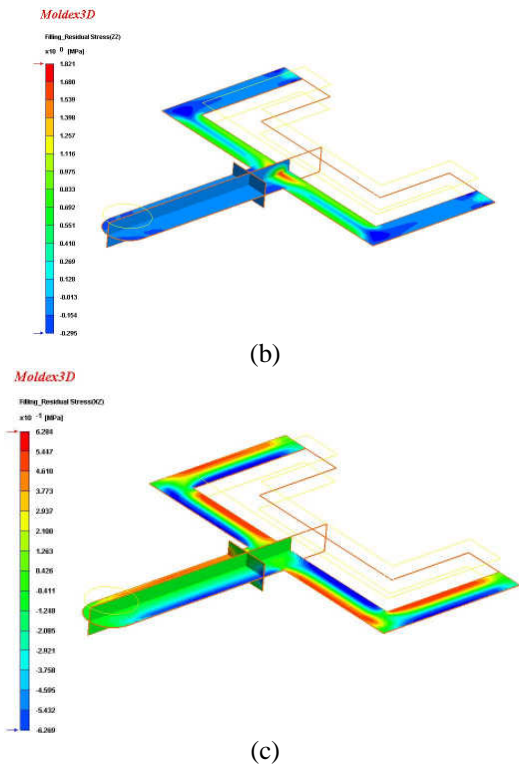


Fig. 5. Residual stresses at main principal directions: (a) T_{xx} , (b) T_{zz} , (c) T_{xy} .

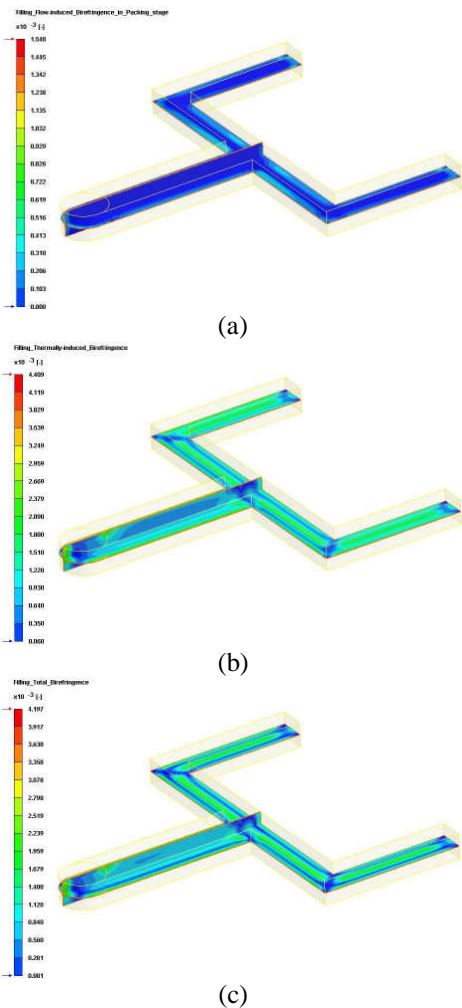


Fig. 6. Birefringence distribution prediction: (a) flow-induced, (b) thermally-induced, (c) total effect.

flow-induced birefringence, (b) thermally-induced birefringence, (c) total birefringence.

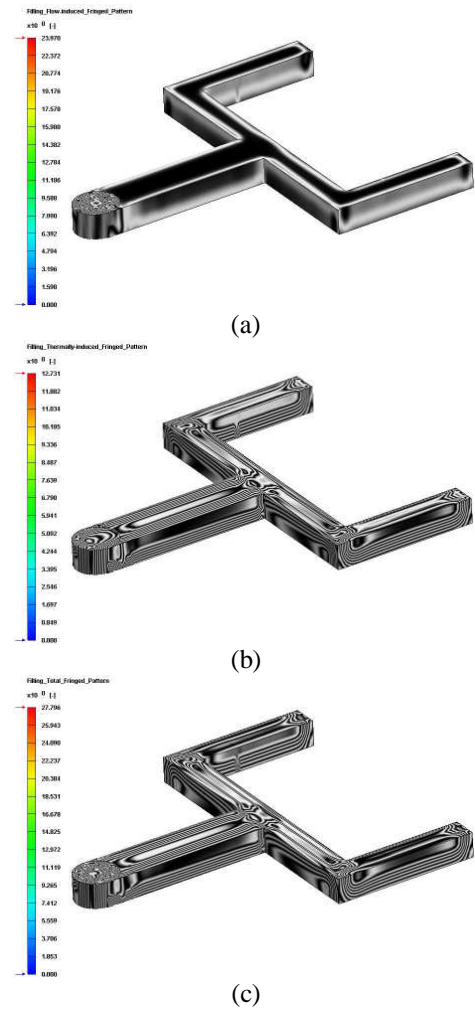


Fig. 7. The fringed pattern: (a) flow-induced, (b) thermally-induced, (c) total effect.

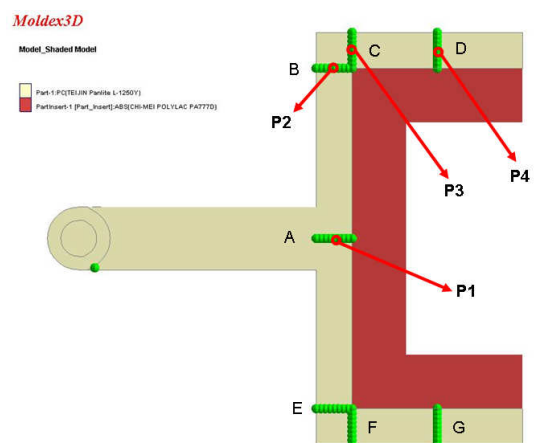
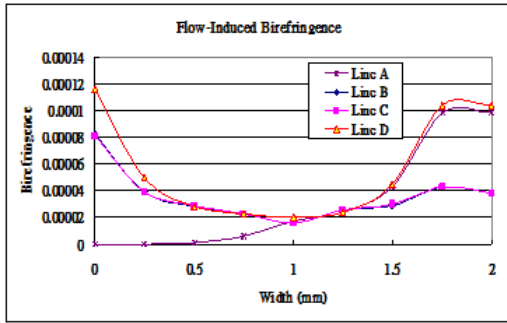
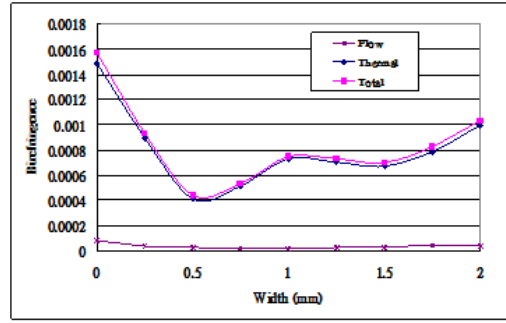


Fig. 8. Residual stresses and birefringence variation study for melt flow from location A to D, where P1 to P4 are at the center points for each line.

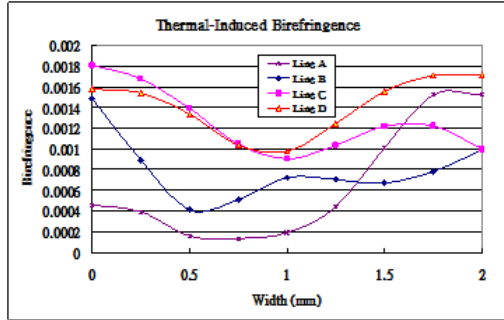


(a)

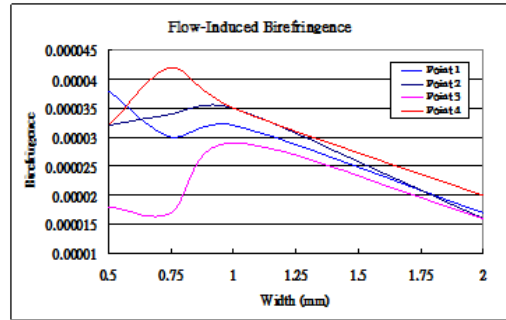


(b)

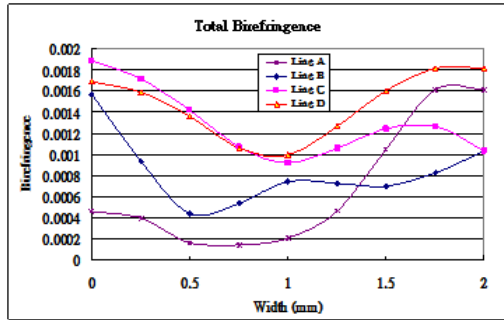
Fig. 10. Birefringence variation along flow direction with $\lambda=0.1$ and width=2.0 mm: (a) Line A, (b) Line B.



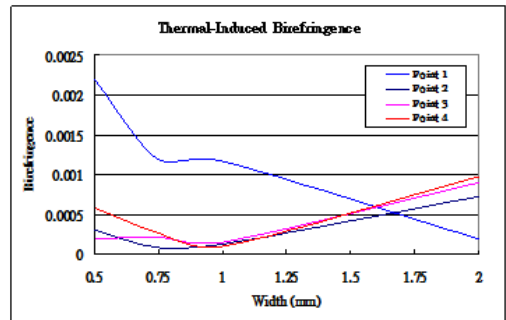
(b)



(a)

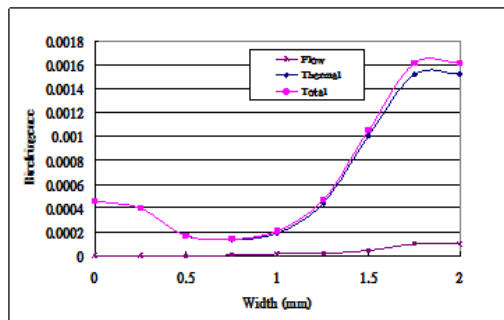


(c)

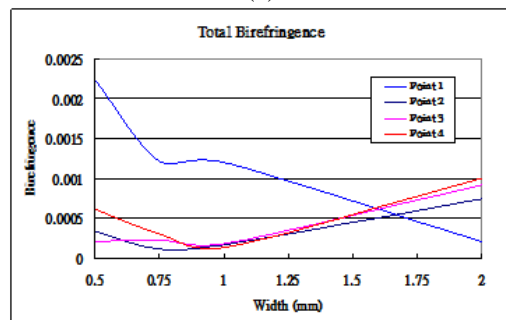


(b)

Fig. 9. Birefringence variation from upstream to downstream when the width is 2.0 mm; where 2.0 mm is located at the interface between melt and the insert. Line A to D are defined in Fig. 8.



(a)



(c)

Fig.11. Birefringence variation along the width increasing: (a) The flow-induced birefringence variation, (b) thermal-induced birefringence variation, (c) total birefringence variation.

Key Words

Sequential multi-component molding, residual stress, birefringence.